

# Topological and Electron-Transfer Properties of Yeast Cytochrome c Adsorbed on Bare Gold Electrodes

Beatrice Bonanni, Dario Alliata, Anna Rita Bizzarri, and Salvatore Cannistraro\*<sup>[a]</sup>

*The redox metalloprotein yeast cytochrome c was directly self-chemisorbed on "bare" gold electrodes through the free sulfur-containing group Cys102. Topological, spectroscopic, and electron transfer properties of the immobilised molecules were investigated by in situ scanning probe microscopy and cyclic voltammetry. Atomic force and scanning tunnelling microscopy revealed individual protein molecules adsorbed on the gold substrate, with no evidence of aggregates. The adsorbed proteins appear to be*

*firmly bound to gold and display dimensions in good agreement with crystallographic data. Cyclic voltammetric analysis showed that up to 84% of the electrode surface is functionalised with electroactive proteins whose measured redox midpoint potential is in good agreement with the formal potential. Our results clearly indicate that this variant of cytochrome c is adsorbed on bare gold electrodes with preservation of morphological properties and redox functionality.*

## Introduction

Metalloproteins have gained considerable interest for their electron transfer (ET) capability, which can be exploited for applications in molecular electronics,<sup>[1]</sup> biosensors and biocatalysis.<sup>[2]</sup> Their natural redox properties and small dimensions make them good candidates for integration in hybrid submicrometer electronic components and novel biosensor configurations.<sup>[3, 4]</sup> The efficient passage of electrons between functional biomolecules and electronic elements is crucial for bioelectronic systems. A key requirement for such applications is the ability to connect redox proteins to electrodes, preferably by chemical bonds, to achieve good electrical contact between the molecule and the conducting substrate. To this end, thanks to the well-known three-dimensional structure and genetic sequence, suitable anchoring groups can be successfully introduced by site-directed mutagenesis.<sup>[5–7]</sup> It is of primary importance that the functionality of the adsorbed protein is preserved.<sup>[8, 9]</sup> Indeed, the controlled adsorption of functional metalloproteins on bare metal electrodes can be very critical: even if many proteins are spontaneously adsorbed on solid surfaces, they may denature or adopt an undesirable orientation, and their inherent electron transfer capability can thus be compromised.<sup>[2, 10, 11]</sup> As an alternative to direct adsorption on bare metal surfaces, electrodes have been modified with a layer of organic molecules<sup>[12–14]</sup> which prevents denaturation of adsorbed proteins and promotes ET by adapting the molecules to a desirable orientation. However, since slower ET is often observed for proteins adsorbed on modified electrodes,<sup>[15, 16]</sup> direct chemisorption of functional proteins on metal surfaces still remains a worthwhile challenge that needs to be characterised in terms of topology, spectroscopy and electron transfer properties, possibly at the single-molecule level. In this vein, we investigated the adsorption of

cytochrome c molecules from the yeast *Saccharomyces cerevisiae* on bare gold electrodes.

Yeast cytochrome c (YCC) is a small (12.5 kDa) single-domain metalloprotein and is an essential component of the mitochondrial respiratory chain that plays a major role in ET between two membrane-bound enzyme complexes, cytochrome c reductase and cytochrome c oxidase.<sup>[17, 18]</sup> A heme-iron redox centre is responsible for the electron transfer function, and iron switches its oxidation state between +2 and +3 in biological functions. The heme group is covalently bound to the protein matrix through thioether linkages involving two cysteine residues. An additional free sulfur-containing group (Cys102) is present in YCC and is suitable for specifically oriented immobilisation on gold by covalent binding,<sup>[19]</sup> as depicted in Figure 1, whereby only minor perturbation of the heme group is expected. Indeed, several works have shown that adsorption of cytochrome c on bare gold electrodes through the cysteine residues directly bound to the heme group (Cys14 and Cys17) is critical, for example, for horse heart cytochrome c (HHCC), which has no additional cysteine residues. On adsorption on gold surfaces, HHCC no longer gives a well-defined and stable electrochemical response, owing to formation of aggregates,<sup>[20]</sup> progressive adsorption of inactive molecules<sup>[21]</sup> or even protein denaturation.<sup>[22]</sup> The presence in YCC of the additional sulfur-

[a] Prof. S. Cannistraro, Dr. B. Bonanni, Dr. D. Alliata, Prof. A. R. Bizzarri  
Biophysics and Nanoscience Group  
INFN, Dipartimento di Scienze Ambientali  
Università della Tuscia, Largo dell'Università  
01100 Viterbo (Italy)  
Fax: (+39) 0761-357179  
E-mail: cannistr@unitus.it

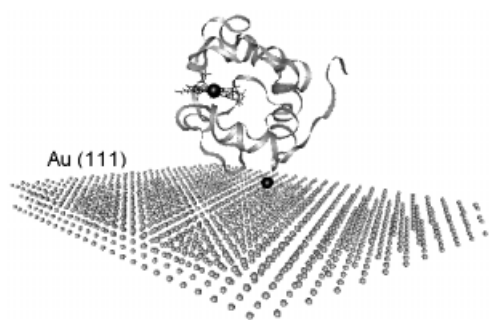


**Figure 1.** Visual Molecular Dynamics (VMD) graphic representation showing YCC adsorption on Au(111) substrate via the sulfur atom of the Cys102 residue. The sulfur atom is represented by the black sphere close to the gold substrate. The heme group is also shown, with the iron atom represented by a black sphere. Coordinates are from X-ray crystallography.<sup>[17]</sup>

containing group that is not directly bound to the heme group makes this protein interesting for direct immobilisation on gold surfaces.

We studied the adsorption of YCC molecules on unmodified ("bare") gold electrodes by integrating high-resolution microscopic techniques, such as scanning probe microscopy (SPM), with cyclic voltammetry. A combination of scanning tunnelling microscopy (STM) and atomic force microscopy (AFM) allowed us to characterise the adsorbed proteins at the single-molecule level and provided information on their electronic properties and morphological characteristics, with particular attention to how the protein molecules are immobilised on the electrode surface and how immobilisation affects their structure. Cyclic voltammetry of YCC on bare gold electrodes was performed to assess the functionality of protein molecules adsorbed on gold substrates. This combination of techniques indicated that YCC molecules adsorbed on bare gold electrodes preserve their morphological characteristics and redox properties.

## Experimental Section

YCC, purchased from Sigma Chemical Co., was used without further purification and dissolved in 1 mM Tris buffer (pH 8.0) to a concentration of 2.6  $\mu\text{M}$ . The solutions were prepared with ultrapure water (resistivity 18.2 M $\Omega$  cm). Substrates (from Arrandee<sup>®</sup>) were vacuum-evaporated thin gold films (thickness 200 nm) on borosilicate glass. Prior to experiments, the substrates were flame-annealed to obtain recrystallised Au(111) terraces. SPM analysis (not shown here) confirmed the presence of atomically flat terraces over hundreds of nanometers, with typical roughness less than 0.1 nm. The annealed Au(111) substrates were directly incubated with the protein solution at 4 °C for times ranging between 30 min and a few hours, both for SPM and cyclic voltammetry experiments. After incubation, samples were gently rinsed with buffer solution to remove any unadsorbed material and immediately immersed in buffer solution for voltammetry measurements and fluid imaging.

AFM images were acquired by a Nanoscope IIIa/Multimode scanning probe microscope (Digital Instruments) equipped with a 12  $\mu\text{m}$  scanner. AFM imaging was performed in buffer solution in tapping mode (TM). The free oscillation of the cantilever was set to approximately 1.2 V; after engaging, the set point was adjusted to

minimal forces. The typical scan rate was 0.6 Hz. Oxide-sharpened silicon nitride probes (Digital Instruments), 100 or 200  $\mu\text{m}$  long, with nominal radius of curvature of 20 nm and spring constants of 0.15 and 0.57 N m<sup>-1</sup>, respectively, were used.

STM experiments were performed with a Molecular Imaging system equipped with a Teflon electrochemical cell and a PicoSTAT bipotentiostat/galvanostat. Samples were measured either under ambient conditions or in electrolyte solution under electrochemical control at a scan rate of about 2 Hz. Typical tunnelling currents were up to 1 nA in air and 10–50 pA in electrolyte solution, with bias voltages of –0.3 and +0.2 V, respectively (positive tip). Electrochemically etched Pt/Ir tips (wax-coated) were purchased from Molecular Imaging Co.

Cyclic voltammetry on YCC monolayers adsorbed on Au(111) was performed with a PicoSTAT bipotentiostat (Molecular Imaging Co.). The electrochemical cell housed two Pt wires as counter- and reference electrodes and was filled with 100  $\mu\text{L}$  of 1 mM Tris electrolyte (pH 8.0). All potentials here are quoted relative to the standard hydrogen electrode (SHE).

## Results and Discussion

The YCC proteins are expected to bind to gold through the free sulfur-containing group Cys102 (as shown schematically in Figure 1), which is readily accessible for chemisorption onto a gold electrode<sup>[23]</sup> while avoiding perturbation of the heme active site. However, we cannot rule out the possibility of electrostatic binding. Indeed, as suggested by Kolb,<sup>[24]</sup> anions in solution may be adsorbed on the gold surface and neutralise, or even overcompensate, the net positive charge of the metal, so that electrostatic adsorption of YCC through positively charged residues is favoured.

The morphology of YCC molecules self-assembled on Au(111) was characterised by a combination of AFM and STM experiments. We found that the density of adsorbed YCC molecules on Au(111) can be varied from very low to full coverage by suitable choice of the incubation time. A representative topography of YCC molecules adsorbed on the Au(111) surface is shown in Figure 2. The sample was incubated for several hours and

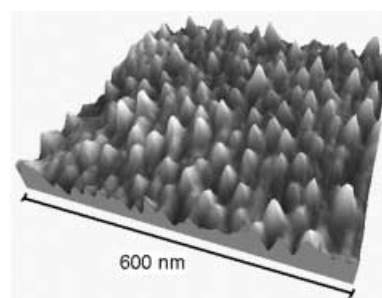


**Figure 2.** Topographic image of YCC molecules adsorbed on Au(111) as recorded by TMAFM in buffer solution. Scan area: 600  $\times$  600 nm, vertical range: 6 nm.

measured by tapping-mode AFM (TMAFM) in buffer solution. Several images similar to that shown in Figure 2, recorded from different areas of the sample, revealed the presence of adsorbed proteins uniformly distributed over the Au(111) surface and with

homogeneous size. The AFM images of adsorbed YCC are stable and reproducible even after repetitive scans; this is typical for robust binding of proteins to gold. Single molecules are well resolved on the gold substrate, as shown in the high-resolution image of Figure 3 a, and there is no evidence for protein mobility on the substrate or formation of aggregates. A representative cross section of a single YCC molecule is shown in Figure 3 b. The molecular height on the gold surface can be estimated from the maximum vertical size. A systematic analysis of cross section profiles for 440 YCC molecules provided a statistical distribution of protein vertical size. The resulting histogram (Figure 4) indicates a monomodal distribution. The mean height of YCC molecules on the gold substrate is 2.6 nm, with a standard deviation of 0.7 nm. This value is close to X-ray crystallographic data,<sup>[17]</sup> and to the value expected for non-denaturing immobilisation on gold through the sulfur atom in the Cys102 residue (about 3.8 nm, as estimated from the topological arrangement corresponding to Figure 1). The standard deviation of the height distribution may be associated with flexibility of the protein on the substrate; a higher probability of protein reorientation is reflected in a broader height distribution. In a comparative study of two poplar plastocyanin mutants, a narrower height distribution was found for anchoring to gold through a disulfide bridge than for anchoring through a single thiol group,<sup>[25]</sup> since the latter binding mode provides for higher flexibility of the adsorbed metalloprotein. The standard deviation estimated for adsorbed YCC molecules ( $\sigma = 0.7$  nm) is closer to the value found for plastocyanin anchored through a single thiol group ( $\sigma = 0.6$  nm<sup>[25]</sup>) and is thus consistent with comparable flexibilities of the two molecules on the substrate.

The typical protein lateral dimension, as evaluated from the full width at half maximum of the molecular cross-section profile (Figure 3 b), is in the range 20–30 nm, considerably larger than the crystallographic data,<sup>[17]</sup> due to the well-known tip broadening. The apparent width  $W$  of a spherical object with diameter  $H$ , imaged by a tip of radius  $r$ , is given approximately by  $W^2 = 8Hr$ .<sup>[26]</sup> For a nominal tip radius of 20 nm and a measured molecular height of 3.3 nm (as in the cross-section profile shown in Figure 3 b) we find  $W = 23$  nm, close to the measured value. However, protein lateral dimensions can be generally recovered by STM imaging,<sup>[6, 25, 27, 28]</sup> which is known to induce less tip

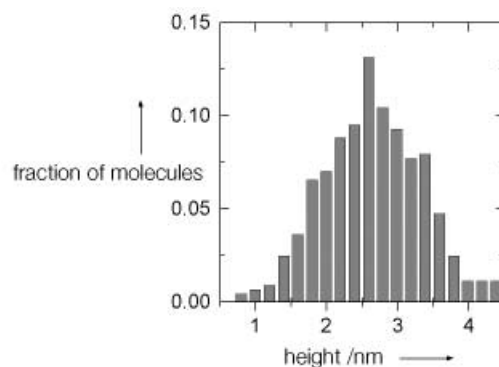


**Figure 4.** Statistical analysis of YCC molecular height on the Au(111) substrate, as measured by TMAFM under buffer solution. The vertical dimension of the proteins was estimated from individual cross-section analysis of 440 molecules. The mean height is 2.6 nm, with a standard deviation of 0.7 nm.

convolution than AFM and often reveals interesting submolecular features.<sup>[6, 29–31]</sup>

Therefore, adsorbed YCC molecules were imaged by STM under ambient conditions. A typical STM image recorded in air from a sample incubated with the protein solution for about one hour is shown in Figure 5 a. The self-chemisorbed proteins are stable and give reproducible images in consecutive scans. To verify the robustness of a single protein–gold bond, the same area was consecutively imaged at different tunnelling currents, from 50 pA up to 1 nA with the bias fixed at  $-0.3$  V. Thus, the tip–protein distance was reduced, that is, the local tip–molecule interaction was increased. Despite this procedure, none of the imaged isolated YCC protein molecules was swept away, and this confirms robust binding of YCC to gold. The typical molecular cross-section profile is shown in Figure 5 b. The full width at half maximum provided estimated YCC lateral dimensions in the range  $4.8 \pm 0.7$  nm, close to that obtained from X-ray crystallography.<sup>[17]</sup> In contrast, the height of adsorbed YCC molecules as measured by STM (0.3–0.5 nm) is notably smaller than the crystallographic size. Considerable reduction in height has been observed in numerous STM images of biomolecules.<sup>[25, 28, 30, 32]</sup> Indeed, STM contrast is not entirely related to the height of the real object. Even if the origin of STM contrast in

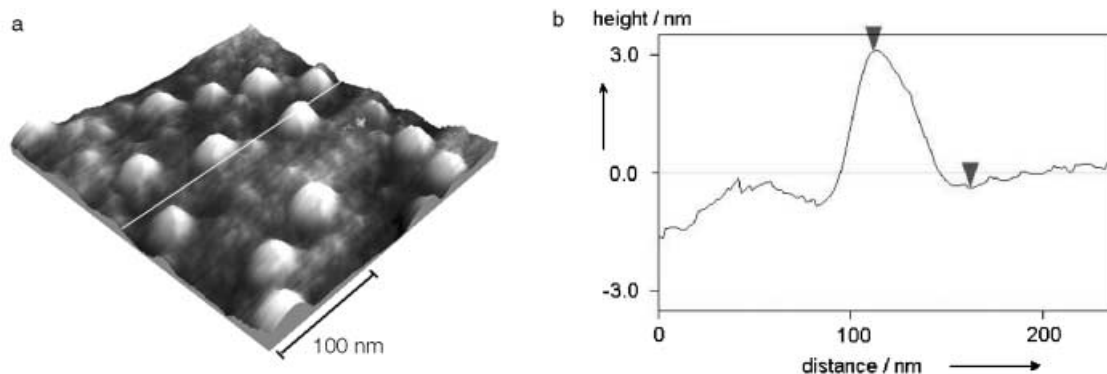


**Figure 3.** a) TMAFM image of YCC molecules adsorbed on Au(111), recorded in buffer solution. b) Representative cross-section profile, recorded along the white line in a). Scan area:  $280 \times 280$  nm, vertical range: 6 nm.

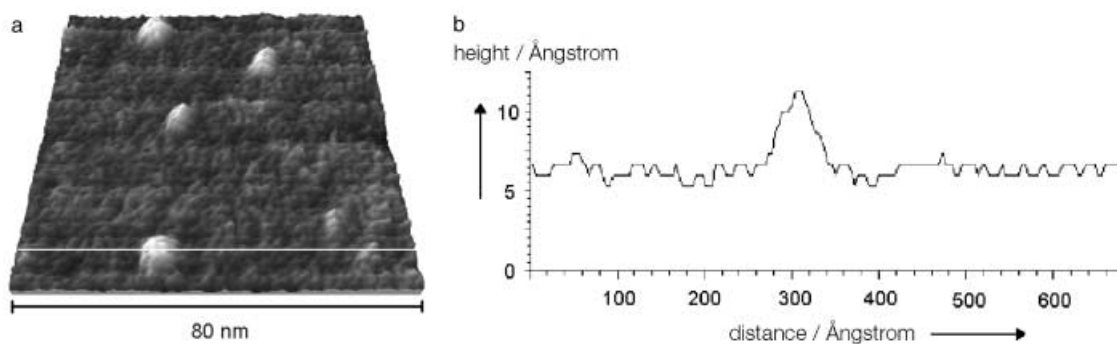


**Figure 5.** a) STM image of YCC under ambient conditions. b) Representative cross-section profile recorded along the white line in a). Scan area:  $80 \times 80$  nm, tunnelling current 100 pA,  $V_{\text{bias}} = -0.300$  V (positive tip), scan rate 1.5 Hz.

protein molecules is still widely debated,<sup>[33–35]</sup> it is well established that STM images are a complex convolution of structural and electronic contributions, so that height data may deviate significantly from purely topographic data. Moreover, in STM, the stress applied by the tip over the molecule is not easily controlled, and possible tip-induced protein compression must be taken into account.

Redox-active molecules can be also studied by in situ STM in electrolyte,<sup>[27, 30, 36]</sup> in which the electrochemical potentials of the two working electrodes involved in the measurement, that is, substrate and tip, are controlled separately. Figure 6 shows an STM image of a single YCC molecule on Au(111) acquired at a substrate potential of 0.265 V versus SHE in buffer solution. Here, the electrochemical potential of the substrate was appositely tuned to a value close to the redox midpoint of the protein (see voltammetry results below). For other metalloproteins<sup>[25, 27]</sup> we recently showed that tunnelling appears to take place in a favoured manner once the substrate potential is properly aligned to the protein redox level. Under these experimental conditions, single YCC molecules are well resolved on the Au(111) substrate (see Figure 6) and there is no evidence of protein aggregates. The adsorbed proteins are not swept away by repetitive scanning, and consecutive STM images are well reproducible with time. This behaviour is at variance with noncovalently adsorbed proteins,<sup>[25, 37]</sup> which instead exhibit

notable mobility over the substrate with consequent evolution of STM images with time. Therefore, our results indicate that YCC molecules are adsorbed on the substrate mainly through covalent binding to gold, likely through the free sulfur-containing group Cys102, even if in principle we cannot completely rule out some involvement of electrostatic interactions in the adsorption mechanism. The quality of STM images of self-chemisorbed YCC single molecules was also tested for different electrochemical potentials of the substrate. For substrate potentials close to the YCC redox midpoint potential (i.e., between 0.150 and 0.380 V versus SHE) the adsorbed molecules remain stable, whereas image quality starts to deteriorate when the electrochemical potential becomes more positive (at a substrate potential of about 0.500 V versus SHE). This apparent sensitivity of the images to the electrochemical potential is consistent with some involvement of protein redox levels in the tunnelling process, as already observed in other redox proteins.<sup>[25, 27]</sup>

The functionality of immobilised YCC on bare gold electrodes was investigated by cyclic voltammetry experiments in which the faradaic current was measured as a function of the substrate potential. The first cycle revealed the presence of two peaks corresponding to the oxidation and reduction of cytochrome c in the native form and a second cathodic peak with a transient behaviour (not shown), which may be consistent with the

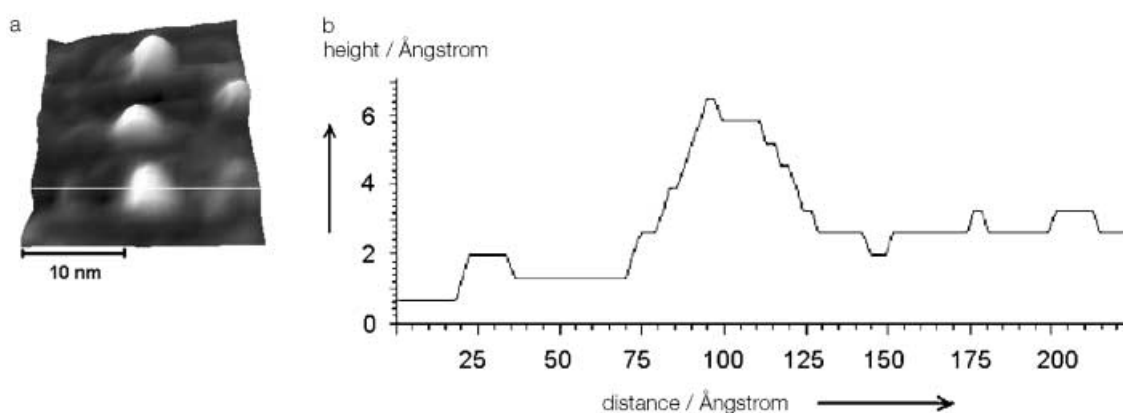


**Figure 6.** a) Isolated YCC proteins chemisorbed on gold substrate, as measured in buffer solution by STM at an electrochemical potential of 0.265 V versus SHE and b) cross-section profile recorded along the white line in a). Scan area:  $24.5 \times 24.5$  nm, tunnelling current 50 pA,  $V_{\text{bias}} = 0.200$  V (positive tip), scan rate 2 Hz.

alkaline form of YCC.<sup>[38]</sup> Figure 7 shows a typical cyclic voltammogram (CV), recorded after 10 cycles, for Au(111) electrodes incubated with YCC solution overnight. The CVs were measured in buffer solution at a voltage scan rate of 50 mV s<sup>-1</sup>. The data

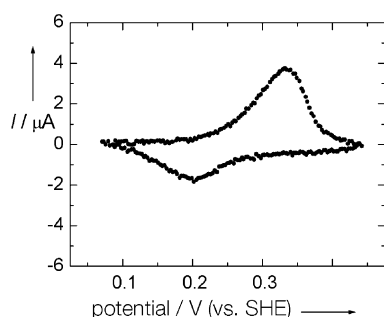


**Figure 7.** Cyclic voltammogram of YCC on Au(111) electrode after subtracting the faradaic current of the bare substrate. Data were recorded in buffer solution at a potential scan rate of 50 mV s<sup>-1</sup>.

shown were obtained after subtracting the faradaic current of the bare Au(111) substrate. The two peaks that can clearly be observed correspond to reduction and oxidation of YCC. The presence of a single anodic and a single cathodic peak is indicative of redox reactions that all occur at a well-defined potential and is consistent with the presence of YCC monomers on the surface.<sup>[20]</sup> The voltammetric response is highly stable, persists in unperturbed form for hours of experimentation and is indicative of a quasireversible electrochemical response. The redox potential, as estimated from the CV, is  $+0.27 \pm 0.02$  V versus SHE, which is in agreement with reported values for cytochrome *c* ( $+0.26 \pm 0.02$  V)<sup>[39]</sup> and close to the value found by this technique for YCC adsorbed on gold-modified electrodes ( $+0.290 \pm 0.002$  V).<sup>[40]</sup>

The anodic and cathodic peaks are separated by 0.075 V, which is quite close to the value expected for an ideal one-electron transfer reaction (0.060 V).<sup>[41]</sup> This is an indication that the electron transfer process is not influenced by direct adsorption on gold, in contrast to what was observed for other types of cytochrome *c* proteins.<sup>[20–22]</sup> The dependence of the peak separation on scan rate was mostly linear up to 1 V s<sup>-1</sup>, which is our instrumental limit.

The heights of anodic and cathodic peaks were monitored as a function of the voltage scan rate (Figure 8). The linear depend-

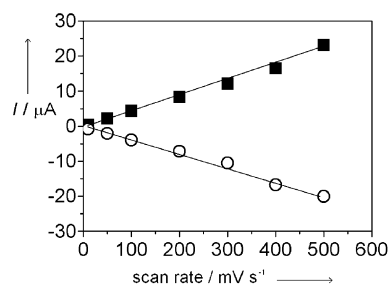


**Figure 8.** Anodic (■) and cathodic (○) peak current *I* versus voltage scan rate, as measured from cyclic voltammograms.

ence of the peak current on the voltage scan rate is consistent with a redox process of an adsorbed species (for a diffusion-limited process a dependence on the square root of the scan rate is expected). An estimate of the surface coverage with electroactive YCC molecules can be obtained from Equation (1)

$$I_p(\nu) = (Nn^2F^2/4RT)\nu \quad (1)$$

where  $I_p$  is the peak current (anodic or cathodic),  $\nu$  is the voltage scan rate,  $N$  is the number of redox-active sites on the surface,  $n$  is the number of electrons transferred,  $F$  the Faraday constant,  $R$  the gas constant and  $T$  the temperature. From the slope of  $I_p$  versus  $\nu$  with  $n = 1$ , we estimate a surface coverage of  $1.21 \times 10^{-11}$  mol cm<sup>-2</sup>. For YCC molecules adsorbed on the electrode surface forming a closely packed monolayer, the surface coverage is expected to be  $1.44 \times 10^{-11}$  mol cm<sup>-2</sup>,<sup>[10]</sup> assuming that all adsorbed molecules have the same size as that obtained by X-ray diffraction.<sup>[17]</sup> Therefore, our data indicate that up to 84% of the electrode surface was successfully functionalised with electroactive proteins. Such a coverage is consistent with that found by scanning probe microscopy on samples incubated overnight. For the 16% missing coverage, as estimated by CV, we cannot exclude some deposition of the alkaline form of YCC at pH 8, even though it is normally observed at pH values higher than 9.<sup>[38]</sup>

To test a possible influence of the buffer conditions on the YCC electrochemical response, as found for other types of cytochrome *c*,<sup>[20, 42]</sup> we performed similar cyclic voltammetry experiments on proteins dissolved in another buffer (phosphate buffer) with different ionic strength (30 mM) and lower pH (pH 7). No evidence for different electrochemical behaviour was found (results not shown). Also with the second buffer, stable and reproducible cyclic voltammograms could be recorded, and the redox midpoint potential was  $0.25 \pm 0.02$  V, a bit lower than the value found in Tris buffer but still comparable to the formal potential. Additionally, the electrode surface coverage was estimated from CV data. For YCC molecules dissolved in pH 7 buffer solution we estimated that 89% of the electrode surface was covered with electroactive molecules. The slightly higher coverage at pH 7 than at pH 8 is consistent with the lower concentration of molecules in the alkaline form as expected at lower pH values.

## Conclusion

We have studied adsorption of YCC molecules on bare gold electrodes, with particular attention to morphological properties and functionality of the adsorbed protein. Extensive characterization of the immobilised proteins at the single-molecule level was achieved by a combination of different techniques. No evidence of molecule aggregates on the gold substrate was found by TMAFM and STM imaging, which instead revealed YCC single molecules firmly bound to gold and no evidence of protein mobility on the substrate, consistent with covalent adsorption of the protein molecules on gold.<sup>[25, 37]</sup> Protein lateral dimensions and height on the gold substrate agree well with

crystallographic data as for non-denaturing adsorption of YCC molecules on bare Au(111) surface.

The redox functionality of YCC molecules immobilised on the gold electrode was assessed by cyclic voltammetry experiments. The voltammetric response of the adsorbed proteins is well defined and stable, and the measured redox potential is in good agreement with the formal potential. Our results clearly indicate a preserved redox functionality of adsorbed molecules, with coverage of up to 84% of the Au (111) electrode substrate. The possibility to adsorb such a high concentration of redox-active cytochrome c with preserved morphological characteristics is of primary importance in view of applications in biosensors and biocatalytic devices.

## Acknowledgements

This work was partially supported by the EC Project SAMBA (V Frame FET), the "Molecular Nanodevices" FIRB project and the "Single Molecule Spectroscopy" INFM-PAIS project.

**Keywords:** chemisorption · metalloproteins · molecular dynamics · scanning probe microscopy · single-molecule studies

- [1] G. Gilardi, A. Fantuzzi, S. J. Sadeghi, *Current Opin. Struct. Biol.* **2001**, *11*, 491.  
[2] I. Willner, B. Willner, *Trends Biotechnol.* **2001**, *19*, 222.  
[3] I. Willner, *Science* **2002**, *298*, 2407.  
[4] C. Joachim, J. K. Gimzewski, A. Aviram, *Nature* **2000**, *408*, 541.  
[5] J. J. Davis, C. M. Halliwell, H. A. O. Hill, G. W. Canters, M. C. Van Amsterdam, M. Ph. Verbeet, *New. J. Chem.* **1998**, 1119.  
[6] J. J. Davis, H. A. O. Hill, *Chem. Commun.* **2002**, 393.  
[7] L. Andolfi, S. Cannistraro, G. W. Canters, P. Facci, A. G. Ficca, I. M. C. Van Amsterdam, M. Ph. Verbeet, *Arch. Biochem. Biophys.* **2002**, *399*, 81.  
[8] K. W. Hipps, *Science* **2001**, *294*, 536.  
[9] X. D. Cui, A. Primak, X. Zarate, J. Tomfohr, O. F. Sankey, A. L. Moore, T. A. Moore, D. Gust, G. Harris, S. M. Lindsay, *Science* **2001**, *294*, 571.  
[10] T. Sagara, K. Niwa, A. Sone, C. Hinnen, K. Niki, *Langmuir* **1990**, *6*, 254.  
[11] I. Taniguchi, K. Watanabe, M. Tominaga, F. M. Hawkridge, *J. Electroanal. Chem.* **1992**, *333*, 331.  
[12] J. Wei, H. Liu, A. R. Dick, H. Yamamoto, Y. He, David H. Waldeck, *J. Am. Chem. Soc.* **2002**, *124*, 9591.  
[13] Z. Salamon, J. T. Hazzard, G. Tollin, *Proc. Natl. Acad. Sci. USA* **1993**, *90*, 6420.  
[14] T. Sagara, H. Murumaki, S. Igarashi, H. Sato, K. Niki, *Langmuir* **1991**, *7*, 3190.  
[15] J. J. Davis, D. Djuricic, K. K. W. Lo, E. N. K. Wallace, L.-L. Wong, H. A. Hill, *Faraday Discuss.* **2000**, *116*, 15.  
[16] X. Chen, R. Ferrigno, J. Yang, G. Whitesides, *Langmuir* **2002**, *18*, 7009.  
[17] G. V. Louie, G. D. Brayer, *J. Molec. Biol.* **1990**, *214*, 527.  
[18] P. Baistrocchi, L. Banci, I. Bestini, P. Turano, K. L. Bren, H. B. Gray, *Biochemistry* **1996**, *35*, 13788.  
[19] R. G. Nuzzo, B. R. Zegarski, L. H. Dubois, *J. Am. Chem. Soc.* **1987**, *109*, 733.  
[20] A. Szucs, M. Novak, *J. Electroanal. Chem.* **1995**, *383*, 75.  
[21] H. Allen O. Hill, N. I. Hunt, A. M. Bond, *J. Electroanalytical Chem.* **1997**, *436*, 17.  
[22] Y. Zhou, T. Nagaoka, G. Zhu, *Biophys. Chem.* **1999**, *79*, 55.  
[23] A. Ulman, *Chem. Rev.* **1996**, *96*, 1533.  
[24] D. M. Kolb, *Angew. Chem.* **2001**, *113*, 1198–1220; *Angew. Chem. Int. Ed.* **2001**, *40*, 1162.  
[25] L. Andolfi, B. Bonanni, G. W. Canters, M. Ph. Verbeet, S. Cannistraro, *Surf. Sci.* **2003**, *530*, 181.  
[26] J. Vesenska, M. Guthold, C. L. Tang, D. Keller, E. Delain, C. Bustamante, *Ultramicroscopy* **1992**, *42*, 1243.  
[27] P. Facci, D. Alliata, S. Cannistraro, *Ultramicroscopy* **2001**, *89*, 291.  
[28] G. B. Khomutov, L. V. Belovolova, S. P. Gubin, V. V. Khanin, A. Yu. Obydenov, A. N. Sergeev-Cherenkov, E. S. Soldatov, A. S. Trifonov, *Bioelectrochem.* **2002**, *55*, 177.  
[29] E. P. Friis, J. E. T. Andersen, L. L. Madsen, P. Møller, R. J. Nichols, K. G. Olesen, J. Ulstrup, *Electrochim. Acta* **1998**, *43*, 19.  
[30] E. P. Friis, J. E. T. Andersen, Y. I. Kharkats, A. M. Kuznestov, R. J. Nichols, J.-D. Zhang, J. Ulstrup, *Proc. Natl. Acad. Sci. USA* **1999**, *96*, 1379.  
[31] P. B. Lukins, T. Oates, *Biochim. Biophys. Acta* **1998**, *1409*, 1.  
[32] Q. Chi, J. Zhang, J. U. Nielsen, E. P. Friis, I. Chorkendorff, G. W. Canters, J. E. T. Andersen, J. Ulstrup, *J. Am. Chem. Soc.* **2000**, *122*, 4047.  
[33] W. Han, E. N. Durantini, T. A. Moore, A. L. Moore, D. Gust, P. Rez, G. Leatherman, G. R. Seely, N. Tao, S. M. Lindsay, *J. Phys. Chem. B* **1997**, *101*, 10719.  
[34] M. Heim, R. Steigerwald, R. Guckenberger, *J. Struct. Biol.* **1997**, *119*, 212.  
[35] S. L. Tang, A. J. McGhie, *Langmuir* **1996**, *12*, 1088.  
[36] N. J. Tao, *Phys. Rev. Lett.* **1996**, *76*, 4066.  
[37] J. E. T. Andersen, P. Møller, M. V. Pedersen, J. Ulstrup, *Surf. Sci.* **1995**, *325*, 193.  
[38] P. D. Barker and A. G. Mauk, *J. Am. Chem. Soc.* **1992**, *114*, 3619.  
[39] G. R. Moore, G. W. Pettigrew, *Cytochrome c: Evolution, Structural and Physicochemical Aspects*, Springer-Verlag, Berlin **1990**, p. 115.  
[40] C. M. Lett, J. G. Guillemette, *Biochem. J.* **2002**, *362*, 281.  
[41] C. H. Hamann, A. Hamnett, W. Vielstich, in *Electrochemistry*, Wiley, New York **1998**, p. 235.  
[42] A. Szucs, M. Novak, *J. Electroanal. Chem.* **1995**, *384*, 47.

Received: April 14, 2003 [F 784]

Revised: June 5, 2003